FEBS Letters 490 (2001) 70–74 FEBS 24589

The role of a proline-induced broken-helix motif in α-helix 2 of *Bacillus thuringiensis* δ-endotoxins

Suzanne Arnold[a], April Curtiss[b], Donald H. Dean[a,b], Oscar Alzate[b,c,*]

[a] *Molecular Genetics Department, The Ohio State University, 484w. 12th Ave., Columbus, OH 43210-1292, USA*
[b] *Biochemistry Department, The Ohio State University, Columbus, OH 43210-1292, USA*
[c] *Universidad Pontificia Bolivariana, Medellín, Colombia*

Received 31 October 2000; revised 10 January 2001; accepted 10 January 2001

First published online 26 January 2001

Edited by Gunnar von Heijne

Abstract ***Bacillus thuringiensis*** **δ-endotoxins (Cry proteins), are widely used for insect control and plant protection. They are water-soluble proteins that insert into membranes forming ion channels. In most Cry toxins α-helix 2 is broken by a highly conserved proline residue (Pro70 in Cry1Ab), generating a broken-helix motif. The flexibility of the motif was altered through site-directed mutagenesis. It was found that increasing the flexibility of the motif decreased the stability, the ion transport ability and the toxicity of the protein. By removing the broken-helix motif, the biological properties were restored to a wild type level.** © **2001 Federation of European Biochemical Societies. Published by Elsevier Science B.V. All rights reserved.**

Key words: Cry protein; δ-Endotoxin; Endotoxin; *Bacillus thuringiensis*

1. Introduction

The physical-chemical properties of proline are among the most important factors determining the membrane-bound state of membrane-translocating proteins. A proline residue is found in all known structures of *Bacillus thuringiensis* (*Bt*) δ-endotoxins, just in the middle of an α-helix, and it is supposed to be present in more than 100 sequenced genes [1]. This amino acid residue induces a broken-helix motif that confers a characteristic structure to domain I in these insecticidal toxins (Fig. 1).

Bt, an endospore-forming bacterium found in natural soils and insect-rich environments, produces insecticidal proteins encased in crystalline inclusions [2]. These crystals dissolve under the conditions of the insect midgut releasing the protoxin forms of the proteins, ranging in molecular weights from 27 to 140 kDa [3]. The digested protoxins yield active δ-endotoxins. The toxin binds to receptors on the surface of the midgut, then forms cation-permeable pores that destroy the trans-epithelial potential, leading to an increase in intracellular pH and death of the insect (for a full review see [3]). Three models have been presented to describe the membrane-bound state of *Bt* toxins. The 'penknife' model, requires α-helices 5 and 7 to flip out of their domain inserting into the membrane as a helical hairpin [4]. The 'umbrella' model suggests that α-helices 4 and 5 or α-helices 6 and 7 insert as a helical hairpin and the other helices flatten out on the membrane surface [5]. A third model, based on antibody affinity and proteinase protection assays leads to the conclusion that the protein inserts as a whole molecule [6–8] and remains confined to the membrane [9].

The Cry1Ab protoxin is digested to a 65 kDa toxin comprised of three domains [10]. Domain I, a 7 α-helices bundle, is believed to be involved in toxin insertion into the membrane [10,11]. The conserved broken-helix motif in α-helix 2, caused by proline 70 (Pro70), generates two α-helices, α2a and α2b (Fig. 1). Although in globular, water-soluble proteins prolines are rarely found mid-helix, mid-helix proline is observed in a large number of membrane-translocating proteins and membrane-intrinsic proteins [12]. Bacteriorhodopsin has proline residues in the middle of three transmembrane α-helices [12], and rhodopsin has proline in five α-helices [13]. The α-helical domain I of diphtheria toxin, has a proline residue (Pro345) between α-helix 8 and 9 [14], involved in the toxin's ability to translocate the membrane [15]. In colicin A, another membrane-translocating protein with an α-helical inserting domain, the proline-caused loop between α-helices 8 and 9 has been proposed to be responsible for insertion into the membrane [16]. The *cis*/*trans* isomerization of proline plays a critical role in the electron transport function of the membrane-protein cytochrome *bc-1* [17].

The present study was aimed to determine the role of the Pro70-induced broken-helix motif in the structure and function of the *Bt* δ-endotoxins. To fulfill this goal, three mutations were designed in Cry1Ab. A proline to alanine mutation (P70A, represents the replacement of a non-polar residue that rigidly fixes the main chain to a small non-polar residue, considered an α-helix former [18]. This was designed to maintain the broken-helix motif without the *cis*/*trans* isomerability expected with proline), a proline to glycine mutation (P70G, expected to increase the flexibility in the α-helix), and the deletion of the 69-Gly-Pro-Ser-71 region (ΔGPS, expected to eliminate the broken-helix motif and induce a single, unbroken α-helix.). The results indicate that rigidity in α-helix 2 is necessary for membrane permeability and toxicity.

2. Materials and methods

2.1. Site-directed mutagenesis, toxin preparation and toxicity assays

Oligonucleotides were from Genemed Synthesis Inc., trypsin was from Sigma, the mutagenesis kit was from Bio-Rad. The *Escherichia coli* clone containing the *Bt* δ-endotoxin gene for Cry1Ab (T. Yama-

*Corresponding author. Fax: (1)-614-292 3206.
E-mail: alzate.2@osu.edu

PII: S0014-5793(01)02139-1

moto, Sandoz Agro Inc., Palo Alto, CA, USA) was used for mutations. Mutagenesis was carried out as described [19]. Sequencing was done with the Dye Terminator Ready Reaction kit (Perkin Elmer) at the Biopolymer facility, The Ohio State University, OH, USA. Purification, activation and analysis of protoxins were performed as described [19].

2.2. Preparation of brush border membrane vesicles (BBMVs)

BBMVs were prepared from fifth instar *Manduca sexta* midguts by the magnesium precipitation method [20]. BBMVs were resuspended in binding buffer (8 mM $NaHPO_4$/2 mM KH_2PO_4/150 mM NaCl, pH 7.4) to a final protein concentration of 1 mg/ml.

2.3. Membrane-partitioning assays

Protease-K and pefabloc were from Boehringer Mannheim. Insertion of toxin into BBMVs was tested by incubating 10 μg of toxin with 100 μg of BBMVs in binding buffer at room temperature for 60 min, after which 50 μg of protease-K was added. After 30 min incubation at room temperature, 50 μg of freshly prepared pefabloc, a protease-K inhibitor, was added to the mixture. The mixtures were spun 30 min later at 13 500 RPM for 10 min. 20 μl of supernatant and the pellet, dissolved in 20 μl binding buffer, were boiled for 5 min after the addition of 5 μl loading buffer [21]. The samples were analyzed with SDS(12%)–PAGE, and the gels stained with Coomassie blue (Pierce). It was expected that toxin inserted in the membrane would be protected from the proteolytic attack of protease-K and thus visible in the gel [7–9].

2.4. Secondary structure analysis

Toxins were purified by HPLC in a Waters625 photodiode array detector with a Bio-Gel/SEC30-XL(300×7.8 mm) size exclusion column (Bio-Rad). The toxin was eluted with pre-filtered 40 mM phosphate buffer, pH 6.8. Conformational changes were determined using circular dichroism (CD) spectroscopy. Spectra were collected in an AVIV-CD2 spectropolarimeter at room temperature in a 1 cm pathlength quartz cell (Hellma) containing 3 ml solution (30 μg toxin in 3 ml Milli-Q water (Millipore)) scanning from 250–200 nm. Data were based on the average of 10 scans.

2.5. Thermal denaturation

Stability of toxins to thermal denaturation was tested using CD at $\lambda = 223$ nm in the range 26–80°C in 2°C increments with 2 min equilibration between scans. 10 μg toxin was analyzed in a Milli-Q water (Millipore)/1.5 M guanidinium hydrochloride solution to aid the denaturation process by lowering the temperature necessary for analysis through the partial chemical denaturation of the toxins. Data were analyzed with SigmaPlot.

2.6. Electrophysiology

Ion transport ability was analyzed by voltage clamping [22]. Experimental conditions and procedures were as described [22], with the small change that the bathing solution was added with 10 mM glycine and the pH adjusted to 7.4, resulting in a more stable signal. Lag time, T_0, was taken as the time necessary for a 10% drop in I_{sc}. Rate of ion transport was determined by the normalized slope of the percent I_{sc} inhibition (μA/min). Analysis of data was performed with SigmaPlot (Jandel Scientific Co.).

3. Results

3.1. Structural analysis

All three mutant protoxins produced stable 65 kDa toxins as Cry1Ab (Fig. 2A, lanes 2–5), indicating that the mutations do not affect toxin expression in *E. coli*. From CD it was found that the ellipticity of the P70A and P70G toxins mirrored the spectra of Cry1Ab, with two distinct minima at 210 and 220 nm (Fig. 3). The ΔGPS toxin's spectrum deviated from the Cry1Ab pattern in the disappearance of the 210 nm minimum and the introduction of an ellipticity minimum at 228 nm. The decrease in ellipticity at 228 nm suggests an increase in α-helical content in the ΔGPS toxin [23].

Analysis of toxins by thermal denaturation stability (Fig. 4), shows that the T_{50} for P70G, P70A and ΔGPS were 72 ± 1.7, 73 ± 1.8 and 78 ± 1.7°C, respectively. Values that overlap with the T_{50} for Cry1Ab (74°C ± 2.5). P70G starts unfolding at a lower temperature, which is probably the result of a more mobile α-helix 2. On the other hand, ΔGPS starts unfolding at a higher temperature than the wild type protein, suggesting that the increase in α-helical contents led to the formation of a more stable structure.

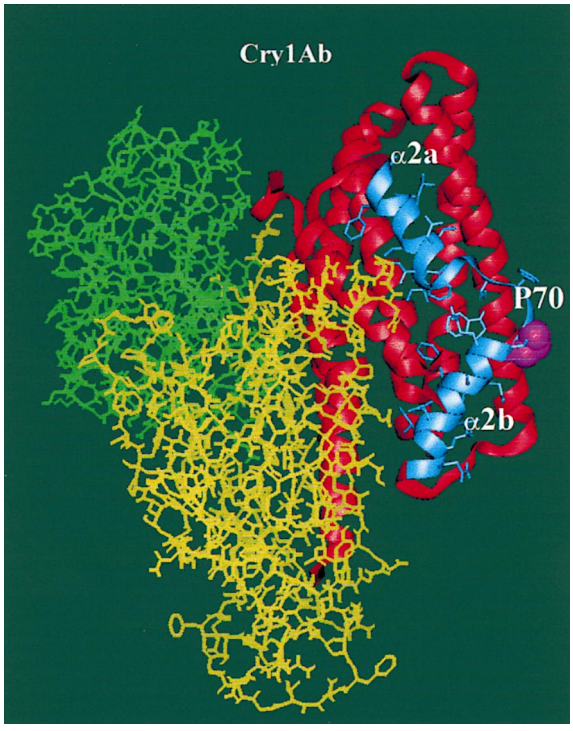

Fig. 1. 3D representation of *Bt* Cry1Ab. 7 α-helical domain I is red. α-helix 2 (helices 2a and 2b) is blue and Pro70 is purple. Domain II is shown in yellow, and domain III in green.

3.2. Toxicity

The ΔGPS and P70A mutant toxins showed no apparent change in toxicity when compared to Cry1Ab (Cry1Ab $LC_{50} = 30.0 \pm 11.9$ ng/cm^2; ΔGPS $LC_{50} = 31.1 \pm 9.5$ ng/cm^2 and P70A $LC_{50} = 42.7 \pm 12.9$ ng/cm^2). The P70G mutant toxin showed about 2–3 fold decrease in toxicity compared to Cry1Ab (P70G $LC_{50} = 81.4 \pm 18.4$ ng/cm^2).

3.3. Electrophysiology

The Lag time in I_{sc} is unaffected by any of the three mutations (Fig. 5). However, the ability of the toxin to disrupt the ion transport rate was markedly affected. Both the P70A (percent $I_{sc} = -2.28$ μA/min) and P70G (percent $I_{sc} = -2.11$ μA/min), displayed decreased ion transport compared to Cry1Ab (percent $I_{sc} = -4.45$ μA/min). The inhibition of I_{sc} by the ΔGPS toxin, (percent $I_{sc} = -4.42$ μA/min), was nearly identical to Cry1Ab.

3.4. Insertion into phospholipid vesicles

The final products of the insertion assays revealed that all three mutants retained the ability to insert into BBMV, shown by the presence of a strong ~60 kDa band found only in the membrane fraction (Fig. 2A). Western blot assays showed

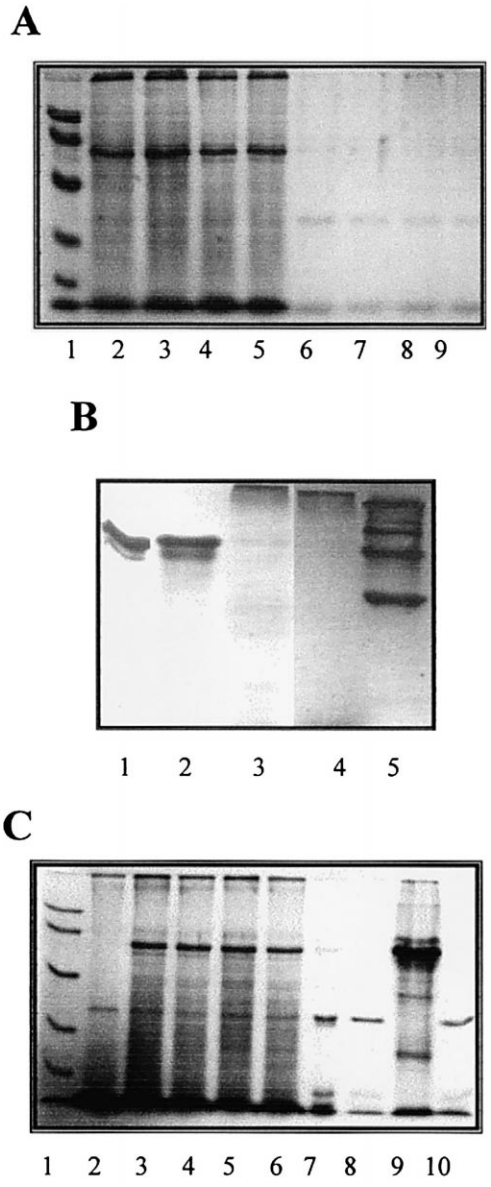

Fig. 2. A: SDS–PAGE analysis of the pellet (lanes 2–5) and the supernatant (lanes 6–9) shows that the protein is protected from digestion by the BBMV. Lane 1: molecular weight marker; lane 2: P70A; lane 3: P70G; lane 4:ΔGPS and lane 5: Cry1Ab; lanes 6–9: corresponding supernatants. B: Non-BBMV inserting proteins. Lane 1: F371C; lane 2: BSA; lanes 3 and 4: corresponding pellets; lane 5: molecular weight marker. C: Controls of the insertion assay on the SDS–PAGE. Lane 1: high range molecular weight marker; lane 2: the experiment as described, without adding toxin (three bands are clear: high molecular weight species, that do not enter the gel; the result of the total digestion, that appears at the bottom of the lane; and a 27 kDa band corresponding to what is left of the protease-K, as deduced from lane 10); lanes 3–6 are repeats of the experiment with the wild type toxin at different incubation times (60, 45, 30 and 15 min, respectively). Lane 7 is the result of a 30 min incubation of the toxin with protease-K showing the degradation of the toxin. Lane 8 is protease-K-incubated with pefabloc, and lane 9 is the wild type toxin used in the assays. Lane 10: protease-K. By comparing lanes 3–6 with lane 10, it is evident that not all the amount of protein used in the assay inserts into the BBMV, which is in strong agreement with the fact that the toxin bound to BBMV determined with ^{125}I-labeled toxin, reaches a saturation point (data not shown).

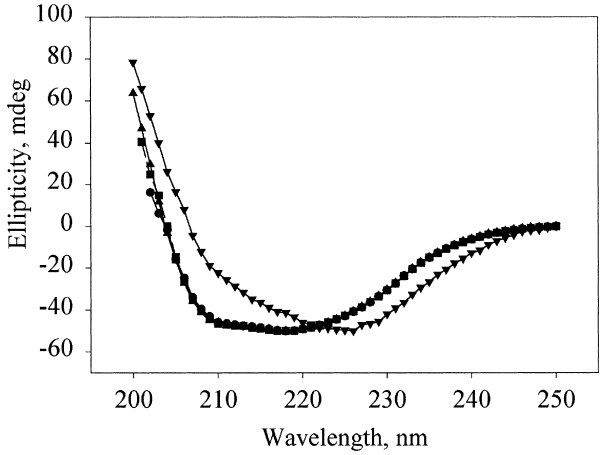

Fig. 3. CD-spectroscopy. The spectra of P70A (■) and P70G (▲) overlap the spectra for Cry1Ab (●), while there are conformational changes in the secondary structure of the ΔGPS (▼).

that this band is due to Cry1Ab toxin [9], the same as the assay without toxin (Fig. 2C, lane 2). Assays with similarly sized non-inserting proteins including bovine serum albumin (BSA) and Cry1Ab-F371C (a mutated non-toxic protein, [24]) indicates that the ~60 kDa toxin band is present only when insertion had occurred. In both cases, the 65 kDa band was absent in the membrane fraction of the final product of the assay (Fig. 2B). Degradation of the Cry1Ab toxin by protease-K was shown by the absence of the 65 kDa band after 30 min incubation (Fig. 2C, lane 7). A final test to assure the insertion into the membrane, and not merely the protection of the toxin by the membrane, was performed by resuspending the membrane fraction of the final product of the insertion assay with solubilization buffer (50 mM sodium carbonate/15 mM dithiothreitol, pH 9.5) followed by 13 500 RPM spin. The pellet and supernatant from this step were analyzed on an SDS(12%)–PAGE gel, stained with Coomassie blue, the ~60 kDa band was again only found in the membrane fraction (data not shown). The ~60 kDa membrane-associated fragment is a truncated form of the 65 kDa toxin, in which 12 amino acid residues from the N-terminal region are missing [8].

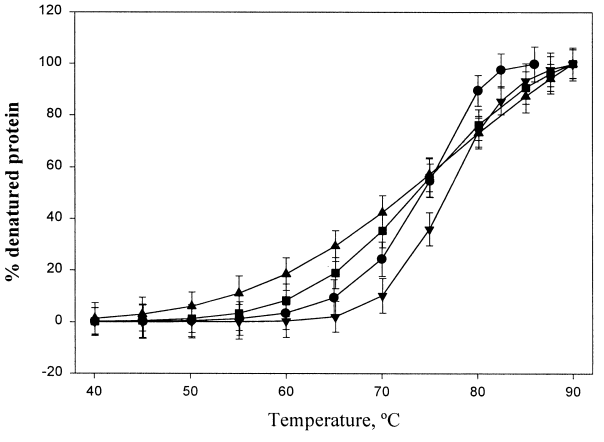

Fig. 4. Thermal denaturation analysis. Cry1Ab (●), P70A (■), P70G (▲) and ΔGPS (▼).

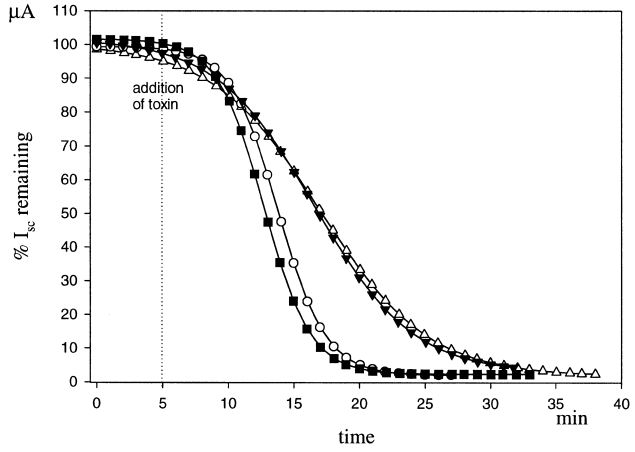

Fig. 5. Ion channel properties of Cry1Ab (■), P70A (△), P70G (▼) and ΔGPS (○) toxins. Dashed line shows the time of toxin injection.

4. Discussion

The broken-helix motif in α-helix 2 (Fig. 1) is highly conserved among Cry toxins and other membrane-inserting proteins. This study focused on the investigation of the role of this motif (caused by Pro70) in the structure and function of Cry1Ab δ-endotoxin. The three mutations – P70A, P70G, and ΔGPS – all resulted in the expression of stable mutant toxins. Secondary structure analysis by CD of the P70G and P70A mutant toxins revealed no conformational changes, suggesting that the replacements of the proline residue by either glycine or alanine maintained the overall secondary structure. CD spectra of the ΔGPS mutant toxin revealed an increase in the α-helical contents of the toxin.

These differences in secondary structure were seen in stability against thermal denaturation as well. ΔGPS was observed to have the same stability as Cry1Ab, consistent with the hypothesized induction of a single, unbroken α-helix 2. The two other mutations caused no detectable change on the T_{50} value, but a slightly earlier start in denaturation, with P70G experiencing a possible greater relative loss in stability than P70A, that could be the result of more flexibility at the mid-helical break in α-helix 2, as the toxin was able to unfold at lower temperature than when the mid-helix break was rigidly held at a specific angle due to the presence of a proline or an alanine residue.

Partition assays indicated that none of the three mutant toxins had lost the ability to insert into the membrane. As indicated by the presence of a ~60 kDa, it is clear that the toxins insert as whole protein (Fig. 2). The conclusion of complete insertion of Cry1Ab agrees with results recently published [8,9]. Although Cry toxins are widely believed only to insert partially, insertion as a whole toxin complex is not a new idea, Wolfersberger et al. presented in 1986 that *B. thuringiensis* toxins inserted into *Pieris brassicae* BBMV as a single molecule [6].

While total insertion of the toxin was unaffected, the mutations did affect the toxin's ion transport ability. Both P70A and P70G showed very similar decreases in their ability to create ion channels suggesting a possible role for the structural conformation resulting from the presence of the Pro70 residue. The expected induction of an unbroken α-helix, as in the ΔGPS mutation, had no effect either on the toxicity or the ability to destroy the membrane potential (Fig. 5), indicating that more flexible residues appear to decrease the ion channel-forming property of the toxin. This recovery of ion channel formation ability by the ΔGPS mutation may be associated with the increase in rigidity of the helix, supported by the thermal denaturation analysis and the CD spectra. It is seen that the broken-helix motif in α-helix 2 in Cry1Ab, which is conserved among several membrane-inserting proteins, including but definitely not limited to other Cry proteins, is involved in structural integrity, which in turns affects the biological activity of the proteins. From this study, Pro70 appears to be necessary for Cry1Ab to insert into phospholipid vesicles in order to have wild type-like lethal activity, by keeping the rigidity of domain I. The Pro70-caused broken-helix motif does seem to have a role in the topological organization of the ion channel in the larval midgut membranes.

Acknowledgements: We thank Cristina Osorio for helping with protein purification and bioassays, and Dr. Douglas Dahlman, University of Kentucky, for providing the *M. sexta* eggs. This work was supported by a NIH Grant to D.H. Dean (Grant # R01 AI 29092). O.A. was a fellow of the Colombian Institution for the Advancement of Sciences (COLCIENCIAS).

References

[1] Crickmore, N., Zeigler, D.R., Feitelson, J., Schnepf, E., Van Rie, J., Lereclus, D., Baum, J. and Dean, D.H. (1998) Microbiol. Mol. Biol. Rev. 62, 807–813.
[2] Höfte, H. and Whiteley, H.R. (1989) Microbiol. Rev. 53, 242–255.
[3] Schnepf, E., Crickmore, N., Van Rie, J., Lereclus, D., Baum, J., Feitelson, J., Zeigler, D.R. and Dean, D.H. (1998) Microbiol. Mol. Biol. Rev. 62, 775–806.
[4] Hodgman, T.C. and Ellar, D.J. (1990) DNA Sequence_I, DNA sequencing and mapping 1, pp. 97–106.
[5] Knowles, B.H. and Dow, J.A. (1993) BioEssays 15, 469–476.
[6] Wolfersberger, M., Hofmann, C. and Lüthy, P. (1986) in: Bacterial Protein Toxins (Falmagne, P., Alouf, J.E., Fehrenbach, F.J., Jeljaszewicz, J., and Thelestam, M., Eds.), Gustav Fischer, Verlag, Stuttgart.
[7] Alzate, O. (1998) Doctoral dissertation, The Ohio State University, OH.
[8] Aronson, A.I., Seng, C. and Wu, L. (1999) Appl. Environ. Microbiol. 65, 2503–2507.
[9] Aronson, A. (2000) Appl. Environ. Microbiol. 65, 4568–4570.
[10] Grochulski, P., Masson, L., Borisova, S., Pusztai-Carey, M., Schwartz, J.L., Brousseau, R. and Cygler, M. (1995) J. Mol. Biol. 254, 447–464.
[11] Li, J., Carroll, J. and Ellar, D.J. (1991) Nature 13, 569–575.
[12] Gennis, R.B. (1986) Biomembranes – Molecular Structure and Function, Springer-Verlag, New York.
[13] Palczewski, K., Kumasaka, T., Hori, T., Behnke, C.A., Motoshima, H., Fox, B.A., LeTrong, I., Teller, D., Okada, T., Stenkamp, R., Yamamoto, M. and Miyano, M. (2000) Science 289, 739–745.
[14] Choe, S.H., Bennet, M.J., Fujii, G., Curmi, P.M.C., Kantardjieff, K.A., Collier, R.J. and Eisenberg, D. (1992) Nature 357, 216–222.
[15] Gray Johnson, V., Nicholls, P.J., Habig, W.H. and Youle, R.J. (1993) J. Biol. Chem. 268, 3514–3519.
[16] Stroud, R.M., Reiling, K., Wiener, M. and Freymann, D. (1998) Struct. Biol. 8, 525–533.
[17] Iwata, S., Lee, J.W., Okada, K., Lee, J.K., Iwata, M., Rasmussen, B., Link, T.A., Ramaswamy, S. and Jap, B.K. (1998) Science 281, 64–71.
[18] Fasman G.D. (Ed.) (1989) Prediction of Protein Structure and the Principles of Protein Conformation, Plenum, New York.
[19] Rajamohan, F., Alzate, O., Cotrill, J.A., Curtiss, A. and Dean, D.H. (1996) Proc. Natl. Acad. Sci. USA 93, 14338–14343.

[20] Wolfersberger, M., Luethy, P., Maurer, A., Parenti, P., Sacchi, F.V., Giordana, B. and Hanozet, G.M. (1987) Comp. Biochem. Physiol. 86A, 301–308.
[21] Sambrook, J., Fritsch, E.F. and Maniatis, T. (1989) Molecular Cloning. A Laboratory Manual, 2nd edn., Cold Spring Harbor Laboratory Press, Cold Spring Harbor, NY.
[22] Harvey, W.R., Crawford, D.N. and Spaeth, D.D. (1990) Methods Enzymol. 192, 599–608.
[23] Andrade, M.A., Chacon, P., Merelo, J.J. and Moran, F. (1993) Protein Eng. 6, 383–390.
[24] Rajamohan, F., Alcantara, E., Lee, M.K., Chen, X.J., Curtiss, A. and Dean, D.H. (1995) J. Bacteriol. 177, 2276–2282.